

Effects of Pore Fluid's pH on the Physico-Mechanical Behavior of High Plasticity Silt

Bhim Kumar Dahal^{1*}, Santosh Pokharel¹, Saroj Basnet¹, Uttam Dahal¹, Shivam Kumar Sah¹, Sneha Neopane¹, Sinam Adhikari¹, Susmita Timalisina¹

¹ Department of Civil Engineering, Pulchowk Campus, IOE, Tribhuvan University, Lalitpur, Bagmati, 44700, Nepal

* Corresponding author's e-mail: bhimd@pcampus.edu.np

ABSTRACT

Acid rain and water pollution are alarming threats, necessitating the study of their influences in different environmental aspects. This study investigates the effects of pore water's pH on the behavior of high plasticity silt. Samples with varied pore fluid pH were tested for Atterberg limits, unconfined compressive strength on the 9th, 18th, and 27th curing days. Particle size distribution and zeta potential were assessed on the 27th day on strength tested samples. The test showed that the soil properties change with the pH of the pore fluid and the days the sample were cured for. The particle size distribution revealed that higher silt and clay fractions were present in acidic and alkaline conditions respectively. Liquid limit varied irregularly with different pH conditions. On all test days, the plastic limit increased under acidic and alkaline conditions compared to neutral conditions. The Unconfined compressive strength and zeta potential were observed to be low in the acidic and alkaline conditions compared to the neutral condition. The result infers that the dissolution of cementitious elements in acidic and alkaline conditions reduces the long-term strength of the soil. These findings encourage geotechnical engineers to evaluate the pH characteristics of the pore fluids during geotechnical analysis.

Keywords: acidity; alkalinity; pH; pollution; soil mechanics; water quality.

INTRODUCTION

In recent decades, there has been a tremendous growth in water pollution, degrading the environment. Underlying causes are industrialisation, contaminants from factory sites, improper waste and wastewater management, uncontrolled landfills, spills, acid rain, and other factors, which changes the chemical nature of soil [Rodríguez-Eugenio et al., 2018]. A conservative worldwide estimate indicates that acidic mine wastewater will adversely harm 20,000 kilometres of river and 70,000 hectares of lake and reservoir area [Schwarzenbach et al., 2010]. Accidental chemical spills and leaks have occurred in the past, and their effects have been examined by some researchers [Al-Omari et al., 2007; Assa'ad, 1998; Rao & Rao, 1994]. Moreover, the chemistry of

rainwater is also changing due to rapid industrialization and air pollution. Many researchers have mentioned the change in pH of rainwater to acidic [Bakhshipour et al., 2016; Hoppe, 1986; Kamon et al., 1997]. Pollutants and acid rains directly affect the subsoil through seepage and infiltration of contaminated water. Most of the time, the soil's pore fluid turns acidic. Other researchers have mentioned the changes in pH of rainwater to alkaline [Yang et al., 2012; Zeng et al., 2020]. Alkaline industrial dumps and the application of limestone to enhance soil properties are some possible causes of the alkaline conditions in soil [Matsumoto et al., 2018]. It is necessary to understand the soil behaviour when subjected to the above-mentioned conditions.

As a developing city, Kathmandu possesses many problems such as tremendous air pollution

leading to acid rain, rapid urbanisation, and unmanaged waste disposal. Vehicle fleets in the valley experienced substantial expansion between 2000 and 2010, growing at a pace of almost 14% annually [Mahapatra et al., 2019]. A high concentration of NO₂ was found at urban sites due to high vehicular activities and SO₂ around the region located within 3km of brick factories [Kiros et al., 2016]. The higher concentration of NO₂ and SO₂ in the atmosphere increases the threat of acid rain. In some locations of Kathmandu valley, the rainwater has been found as acidic (pH 5.04) while in others is alkaline (pH 8.07) [Shrestha et al., 2013]. These findings necessitate the study of the behaviour of Kathmandu soil subjected to change in pore fluid's pH.

Different soils behave differently upon the same phenomena due to mineralogical, and physical variations. It can be observed by contrasting results obtained by different researcher in this field, which is discussed further. Moreover, the need is demanding but limited studies have been done on this topic. This study tries to explore the behaviour of soil on exposure with pore fluid of different pH conditions. For this, the zeta potential, particle size distribution, Atterberg limits, and unconfined compressive strength of Kathmandu's highly plastic silty soil were examined in relation to the pore fluid's pH. It will help to understand the impact associated with ongoing water pollution on important soil behaviour and fill the knowledge gap to some extent.

BACKGROUND

The principal factors influencing fine-grained soil behaviour are clay mineralogy, cation exchange capacity, specific surface area, and clay percentage [Sivapullaiyah, 2015]. The modification of pore fluid's pH has a major impact on these factors. Mineral dissolution and changes in the thickness of the diffuse double layer are the main physical and chemical events. In dry clay, cations such as Ca²⁺, Mg²⁺, Na⁺, and K⁺ that surround the particles and are held by electrostatic attraction balance the negative charge of the clay particles. These cations and a few anions float around the clay particles when water is added. This configuration is called the diffuse double layer (DDL) [Das, 2010]. According to Mitchell & Soga (2005), the thickness of DDL is:

$$\frac{1}{K} = \left(\frac{\epsilon_0 DkT}{2n_0 e^2 v^2} \right)^{1/2} \quad (1)$$

where: K is the thickness of DDL,
 ϵ_0 is the permittivity of the vacuum
 D is the dielectric constant,
 k is Boltzmann's constant,
 n_0 is the electrolyte concentration of the medium,
 e is the electronic charge,
 v is cation valence.

It may be deduced from the expression that, other factors being constant, the thickness varies inversely with valence and square root of concentration and directly with square root of dielectric constant and temperature. The extent of a double layer is reduced as a result of lowering pH, which also increases the positive charges on clay particles, decreasing the inter-particle repulsion [Hoppe, 1986]. It causes the formation of bigger clay aggregates with closer-packed clay particles [Gratchev & Towhata, 2013]. The likelihood of H⁺ ions from the hydroxyl to enter the solution increases with increasing pH, as does the effective negative charge of the particles [Mitchell & Soga, 2005]. It leads to an increase in the thickness of the DDL. Moreover, the thickness of DDL is also influenced by types of exchangeable ions. Na-treated clay produces thicker DDL in comparison with Ca-treated clay [Abdullah et al., 1999]. Cations of one type can replace cations of another type. The relative abundance of the various ion types, valence, and ion size all have a significant role in the ease of replacement [Mitchell & Soga, 2005].

The presence of both monovalent and polyvalent ions affects the diffuse double layer, resulting in variations in electrophoretic mobility, which alter the zeta potential [Lowry et al., 2016]. Zeta potential, which describes the properties of solid/liquid and liquid/gaseous interfaces, is an important parameter for electrical double layers [Salopek et al., 1992]. The zeta potential can be used as an indicator for the electrical characteristics of the clay water-electrolyte system since it exhibits the effects of clay mineralogy, size, charge, and electrolyte composition [Shang, 1997]. As the pH of the solution is raised, the membrane's zeta potential frequently shifts from positive to negative, impacting the deposition of charged particles on the membrane surface [Ismail et al., 2019].

Furthermore, the dissolution of minerals increases due to alterations in the characteristics of the pore fluid that affect the effective charge on the mineral surface [Santamarina et al., 2001]. Figure 1 shows the dissolution of alumina and silica at different pH conditions. The dissolution of alumina occurs in both acidic and alkaline conditions exhibiting its amphoteric nature, whereas the dissolution of silica occurs in alkaline conditions. The solution chemistry of aluminium has a significant influence on the chemical behavior of clay [Hoppe, 1986]. The Al^{3+} ion occurs predominantly below pH 4.7, and $\text{Al}(\text{OH})_4^-$ above pH 8 [Hoppe, 1986]. Al^{3+} aids in aggregation of particles in solution whereas $\text{Al}(\text{OH})_4^-$ doesn't induce particle aggregation [Matsumoto et al., 2018]. Another significant phenomenon that takes place when pore fluid changes from neutral to acidic or alkaline is the dissolution of carbonate and amorphous bonding. SiO_2 , Al_2O_3 , and Fe_2O_3 are the main cementing agents in soil which can react in either an acidic or an alkaline environment [Xu et al., 2021]. A loose soil structure is formed when the cementing agents between clay particles are destroyed by the acidic solution, resulting in a structure with more voids and a higher clay liquid limit [Abedi Koupai et al., 2020].

In past studies, pH of pore fluid has altered the particle size distribution of soils due to aggregation and dissociation of the clay cluster. Clay fraction and silt fraction were found to be decreased at lower and higher pH respectively [Matsumoto et al., 2018; Xiu-juan et al., 2018]. Y. Li et al. (2021) have obtained an increase in clay content with both time and pH on laterite

soil. Atterberg limits were also found to be affected by the pore fluid's pH. Abedi Koupai et al. (2020) and Osuolale et al. (2012) were conclusive that the liquid limit increased with low or high-pH pore fluid. Opposite conclusions were given by Matsumoto et al. (2018) and Spagnoli et al. (2012). Sunil et al. (2006) reported that the liquid limit of laterite soil increased under acidic conditions (pH 5) while decreased under basic conditions (pH 8). Kamon et al. (1997) observed that the liquid limit and the plasticity index increased with soaking time and also with decreasing pH levels of artificial acid rain. The plastic limit of soil was less affected by the acidic or alkaline nature of pore fluid [Kamon et al., 1997; Matsumoto et al., 2018]. However, Umesha et al. (2012) found an increasing trend in plastic limits up to 5% and then decreasing in black cotton soil when treated with different concentrations of acids.

The pore fluid pH affected unconfined compressive strength (UCS) in many past studies. Abedi Koupai et al. (2020) found that clayey soil's UCS rises when pore fluid gets more acidic or alkaline. In some studies, UCS decreased when the soil sample was soaked [Sunil et al., 2006] or infiltrated [Bakhshipour et al., 2016] with acidic fluid. Liu et al. (2021) found that acidic fluids have weakening effects on loess's UCS when exposed to hydrochloric, sulfuric, and nitric acid of different concentrations. Khodabandeh et al. (2020) found a reduction in UCS of loessial soil when exposed to both acidic and alkaline solutions. Ashfaq et al. (2019) found a decrease in UCS of black cotton and kaolinite soil with curing days on treatment with NaOH .

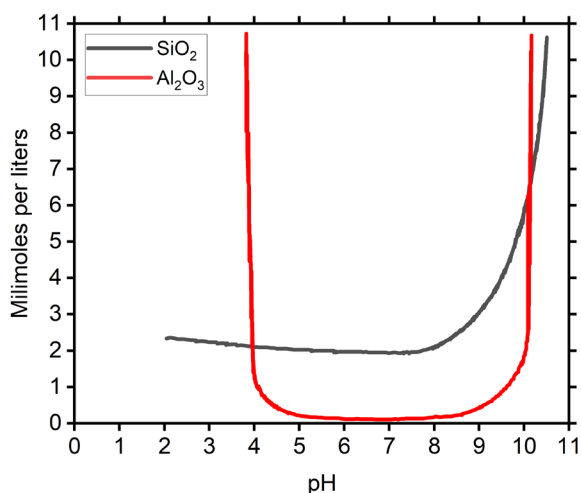


Figure 1. Solubility of silica and alumina, after Hoppe (1986)

METHODOLOGY

The research was conducted on the soil available at the central material testing laboratory, Pulchowk campus. The conceptual framework of the research is presented in Figure 2 and elaborated in the subsequent sections hereunder.

Test material

Before examination, the soil was crushed, air-dried, and sieved through a 425-micron sieve to create a homogenous sample. IS Standards were considered for laboratory works. According to IS:2720-3/1 (1980), IS:2720-4 (1985) and IS:2720-5 (1985), respectively, specific gravity

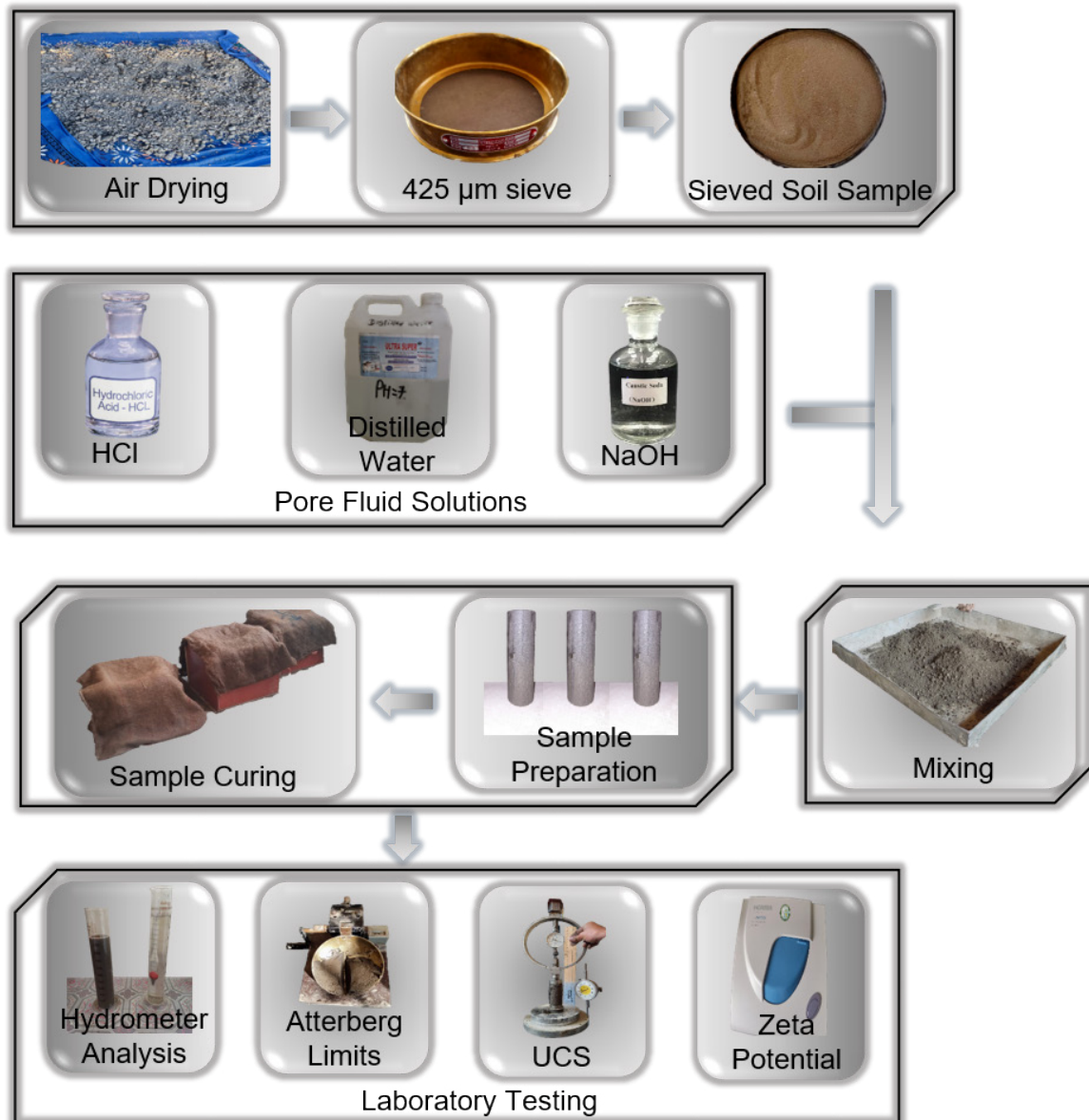


Figure 2. Conceptual framework

tests, grain size analyses, and Atterberg limit tests were carried out to determine the soil parameters. Figure 4 depicts the soil's distribution of grain sizes. According to the IS soil classification system [IS 1498, 1970], the soil is high plasticity silt (MH). The Standard Proctor Compaction Test was used to obtain the optimum moisture content and maximum dry density of the soil. Using a pH meter (0.1), the original sample's pH was calculated at a soil-to-water ratio of 0.4 g/ml in accordance with IS:2720–26 (1987). Table 1 contains a description of the original soil's characteristics. By utilizing HCl and NaOH, the pH of the pore fluid was adjusted to 3 and 10, respectively. The pH of distilled water used was 6.5.

Sample preparation

For the sample preparation for Atterberg limits and the unconfined compression test, air-dried soil was mixed with pore fluid maintaining optimum moisture content ($W_{omc} = 30\%$), thus obtaining the mixed sample. The mixing was done in a PVC bucket to avoid any chemical reaction of acidic and alkaline solutions with the apparatus. The adoption of a mixing approach, which provided a homogeneous pore fluid concentration in the soil sample rather than leaching the samples with pore fluid, prevented the creation of a metastable soil structure [Ratnaweera & Meegoda, 2006]. The mixed sample was subjected to curing

Table 1. Properties of original soil

Soil properties	
Liquid limit	50.82%
Plastic limit	34.36%
Plasticity index	16.46%
Specific gravity	2.568
Maximum dry density	1.4 g/cc
Optimum moisture content	30.20%
pH	7.3
UCS	187.6 kPa
D ₆₀	0.067 mm
D ₃₀	0.011 mm
D ₁₀	0.004 mm

and the Atterberg limit test was conducted on different curing days using distilled water after that. For the UCS test, samples were prepared using mixed sample compacting initially using Harvard Miniature Compaction Apparatus, having 70 mm height and 31mm diameter and UCS samples were subjected to curing. Samples were tested for 27 days in equal intervals of 9 days. Particle size analysis and zeta potential measurement were performed on UCS tested samples after 27 days of curing. The tested samples were air dried and the wet sieve and hydrometer analysis was conducted, avoiding the crushing and grinding of the sample. The curing of samples was done by storing them in a sealed PVC bucket covered with a damp jute gunny bag. Figure 3 shows the

initial mass of the UCS samples during preparation and before the UCS test. In this study, the variation of mass of samples due to moisture loss is within 5%.

Laboratory testing

The samples were tested at zero, on the 9th, 18th, and 27th days. Since soil properties change over time during the curing process, maintaining consistent intervals between testing periods enhances the visibility of these variations. This approach also enables equitable time-based comparisons of the results. For particle size distribution, the wet sieve and hydrometer analysis was performed. The specific gravity of the original oven dried sample was determined by a pycnometer test. Percussion method was used to test the liquid limit in accordance with IS:2720–5 (1985). The UCS test of all the prepared samples was performed in a UCS testing machine at a uniform strain rate of 1.25 mm/min as per IS:2720–10 (1973).

The XRD analysis was done with an X-ray diffractometer (Bruker D2 Phaser) using an X-ray beam (Cu-Kα) of wavelength 1.54060 Å for mineralogical analysis. The observation was taken for 2θ starting from 10° to 90°. The zeta potential of the original and UCS-tested sample after 27th days was also determined by using a nano-particle analyser (SZ-100V2). For the determination of zeta potential, 10 mg of soil passing through

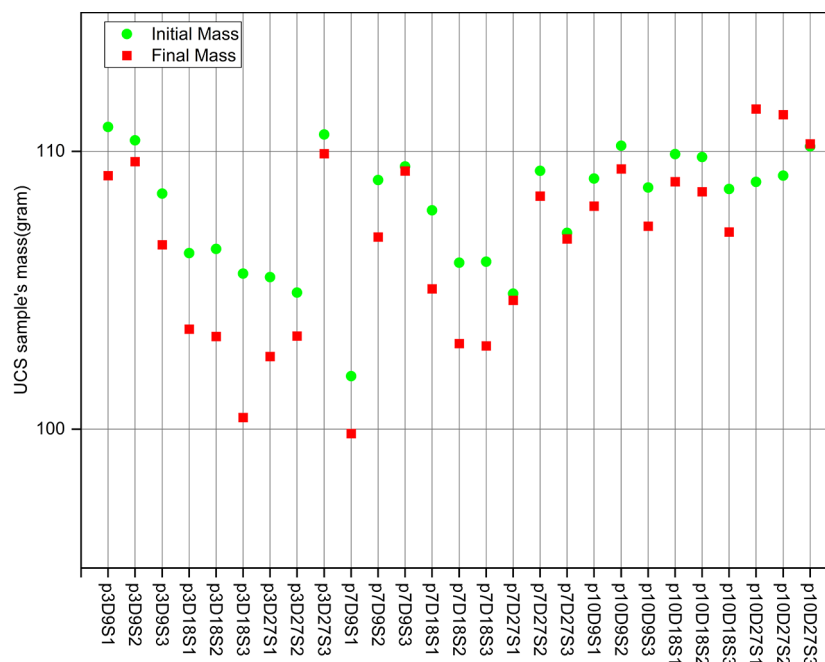


Figure 3. Variation of mass of UCS sample before and after curing

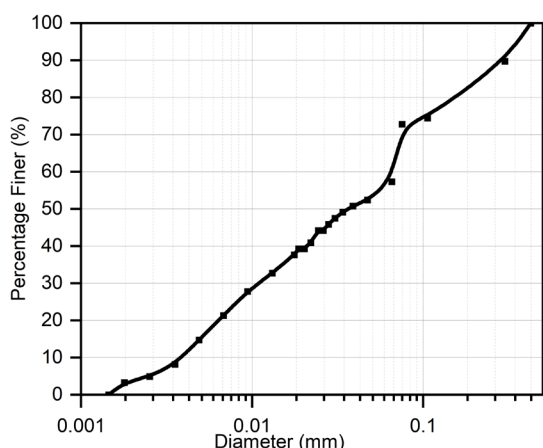


Figure 4. Particle size distribution of original soil

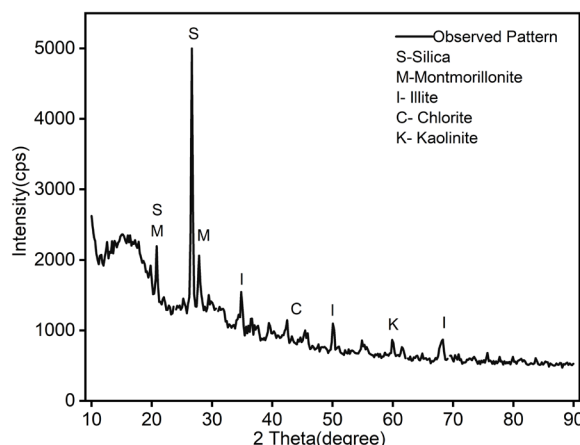


Figure 5. XRD pattern on original soil

425 microns was taken and dissolved by stirring in 40 ml (250 mg/l of concentration) of distilled water with the help of a magnetic stirrer for 10 minutes. Soil suspension’s pH was determined and zeta potential was measured.

RESULTS AND DISCUSSION

Mineralogical analysis and zeta potential

The result of XRD analysis on the original soil is shown in Figure 5. The obtained XRD data were interpreted with ‘MATCH 3.14 Build 233’ software. The relative percentage composition is shown in Figure 6. Quartz (Silica) was found to be the major constituent mineral in the sample. Among clay minerals, Illite was present in the largest fraction, followed by Montmorillonite, Chlorite, and Kaolinite. The result of zeta potential is shown in Table 2. The zeta potential of soils in acidic and alkaline conditions decreased, as compared to the neutral condition. DDL theory can be used to explain how clay mineral zeta potential changes over a large pH range [Nikhil John & Arnepalli, 2019]. Higher H⁺ ion concentrations in the solution and H⁺ ion adsorption onto mineral surfaces in an acidic environment compress the diffuse electrical double layer, lowering zeta potential values. While in alkaline conditions, the amount of OH⁻ ions in the solution rises and they bind to mineral surfaces to form a thick, diffuse electrical double layer that raises the zeta potential [Chorom & Rengasamy, 1995; Yukselen & Kaya, 2003]. This study found that soil’s zeta potential was lower in acidic than in neutral conditions, which is well in line with previous research. The literature is defied by the outcome under the

alkaline situation, when the zeta potential is actually lowered. But Nikhil John & Arnepalli (2019) also found that the zeta potential was reduced in alkaline pH. The reduction results from the clay minerals’ dissolution at high pH. The high valency minerals dissolved into the solution when the soil was treated with alkaline fluid for 27 days prior to the measurement, influencing the DDL thickness and lowering the zeta potential since mineral dissolution is a time-dependent process [Nikhil John & Arnepalli, 2019]. The zeta potential of soil treated with distilled water decreased significantly in comparison to untreated original soil. Moreover, the pH of soil suspension (250 mg/l) measured before zeta potential measurement for the original soil is higher than that of cured samples at different pH conditions. This might be attributed to aging effects [Lessard & Mitchell, 1985]. According to Lessard & Mitchell (1985), while samples are aging, organic material is oxidized to produce carbonic acid in the

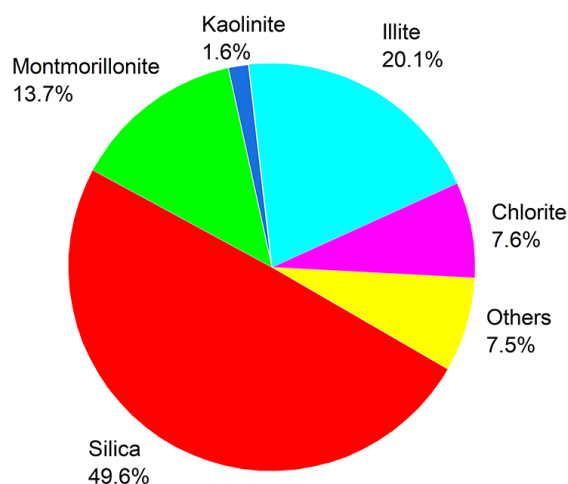


Figure 6. Mineralogical distribution of original soil

Table 2. Zeta potential results

Soil sample	pH of soil suspension (before zeta potential measurement)	Zeta potential (mV)
Original	7.0	-114.5
Acidic	5.6	-32.2
Neutral	6.1	-46.8
Alkaline	6.6	-23.6

presence of oxygen. In addition, sulfuric acid is created through the oxidation of pyrite and iron mono-sulfide. Both sulfuric and carbonic acids dissolve calcium carbonate, raising the amount of calcium ions in the pore water as a result. The diffuse double layer absorbs a significant percentage of the dissolved calcium, which pushes sodium, potassium, and magnesium out of the adsorbed system and into the free pore water. The presence of calcium ions in the diffuse double layer decreased the zeta potential. In this study, pH of original uncured soil suspension is obtained to be higher than that of cured sample. The reduction in soil’s pH with aging has also been observed in some past studies [Ogner et al., 2001; Prodromou & Pavlatou-Ve, 1998; Yue et al., 2022]. The reduction in soil pH observed in this study shows the occurrence of an aging effect during

the curing of the sample. Moreover, in alkaline condition, OH⁻ ion is consumed for dissolution of silica and alumina, thereby reducing the pH concentration [Al-Taie et al., 2018; Ola, 1980].

Particle size distribution

The particle size distribution depicted in Figure 7 was produced after particle size analysis was performed on UCS tested samples that were collected after 27 days. Table 3 illustrates how clay and silt fractions vary with pH. The soil in acidic and neutral conditions showed lower clay fraction as compared to alkaline condition. This showed the occurrence of particle dissociation during the alkaline condition and particle aggregation during the acidic condition, resulting in a higher silt fraction. This is also supported by the suspension behaviour of the original soil at acidic, neutral and alkaline pore fluids shown in Figure 11. These results agree with results obtained by Matsumoto et al. (2018), Xiu-juan et al. (2018) and Y. Li et al. (2021). In acidic condition, aluminium primarily exists as Al³⁺ and, Al³⁺ being an aggregating agent, it aggregates the soil particles. This increased soil particle size, thereby decreasing clay content and increasing silt content [Matsumoto et al., 2018]. However, in the alkaline setting, the majority of the Al is present as Al(OH)⁴⁻, hence particle aggregation was not triggered. Additionally, the hydrogen ions in an acidic environment enhance the positive charge on the clay surface, which diminishes the thickness of the diffuse double-layer and increases the forces of inter-particle attraction that lead to particle aggregation. Furthermore, the hydroxyl ions in the alkaline solution react

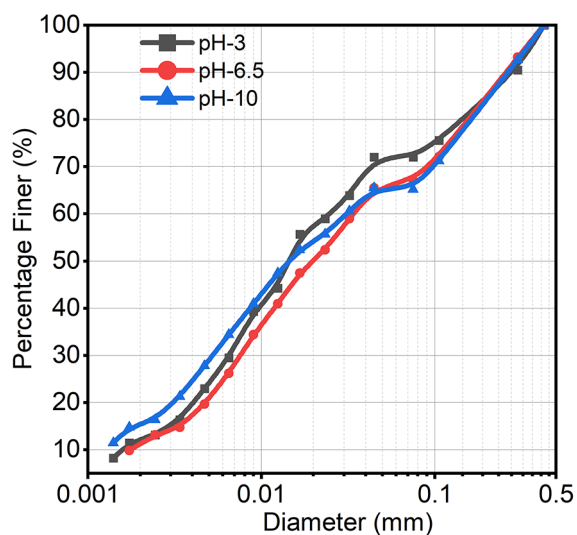


Figure 7. Particle size distribution after subjected to curing for 27 days

Table 3. Clay and Silt contents of soil sample subjected to curing for 27 days

pH	Clay fraction, d<2 μm (%)	Silt fraction, 2 μm ≤ d < 75 μm (%)
3	12.17	60.67
6.5	11.28	56.65
10	15.47	51.07

with the cations, which speeds up the particle decomposition [Xiu-juan et al., 2018].

Atterberg limits

Figures 8(a) and 8(b) shows the variation of Atterberg limits with pH. There is an insignificant change in liquid limit concerning pH at day zero test. The liquid limit increased for acidic condition compared to neutral and alkaline conditions on the ninth day. For the day eighteen test, an increase in the liquid limit for both acidic and alkaline conditions was obtained. Similar results were obtained by Abedi Koupai et al. (2020) and Osuolale et al. (2012). The addition of acidic fluid to soil dissolved cementing agents between soil particles, producing structures with larger voids, forming loose structures and resulting in the greater liquid limit of the clay. Higher liquid limit values compared to distilled water were produced by adding alkali solution because it increased soil manipulation (due to extra ions, pH fluctuations, and the formation of new inter-particle

face-to-face connections) [Abedi Koupai et al., 2020]. For the day 27 test, there is an opposite trend in liquid limit i.e. low liquid limit at acidic condition compared to neutral condition. Similar results were obtained by Matsumoto et al. (2018) and Spagnoli et al. (2012). Moreover, this trend is also compatible with the trend of measured zeta potential and obtained particle size distribution. The amount of water held as double-layer water is indicated by the liquid limit [Spagnoli et al., 2012]. Narrower DDL causes the clay particle to aggregate, forming a more compact structure and hence lower liquid limit at acidic condition. Though some researchers mentioned little changes in plastic limit with pore fluid’s pH, significant variation in plastic limit with pH was obtained in this study. The plastic limit increased at acidic and basic conditions. [Umesha et al., 2012] also found an increase in the plastic limit up to 5% of acid concentration on black cotton soil in their study. The variation of Atterberg limits with curing days are seen in Figures 8(c) and 8(d). With curing days, there was a tendency for both the

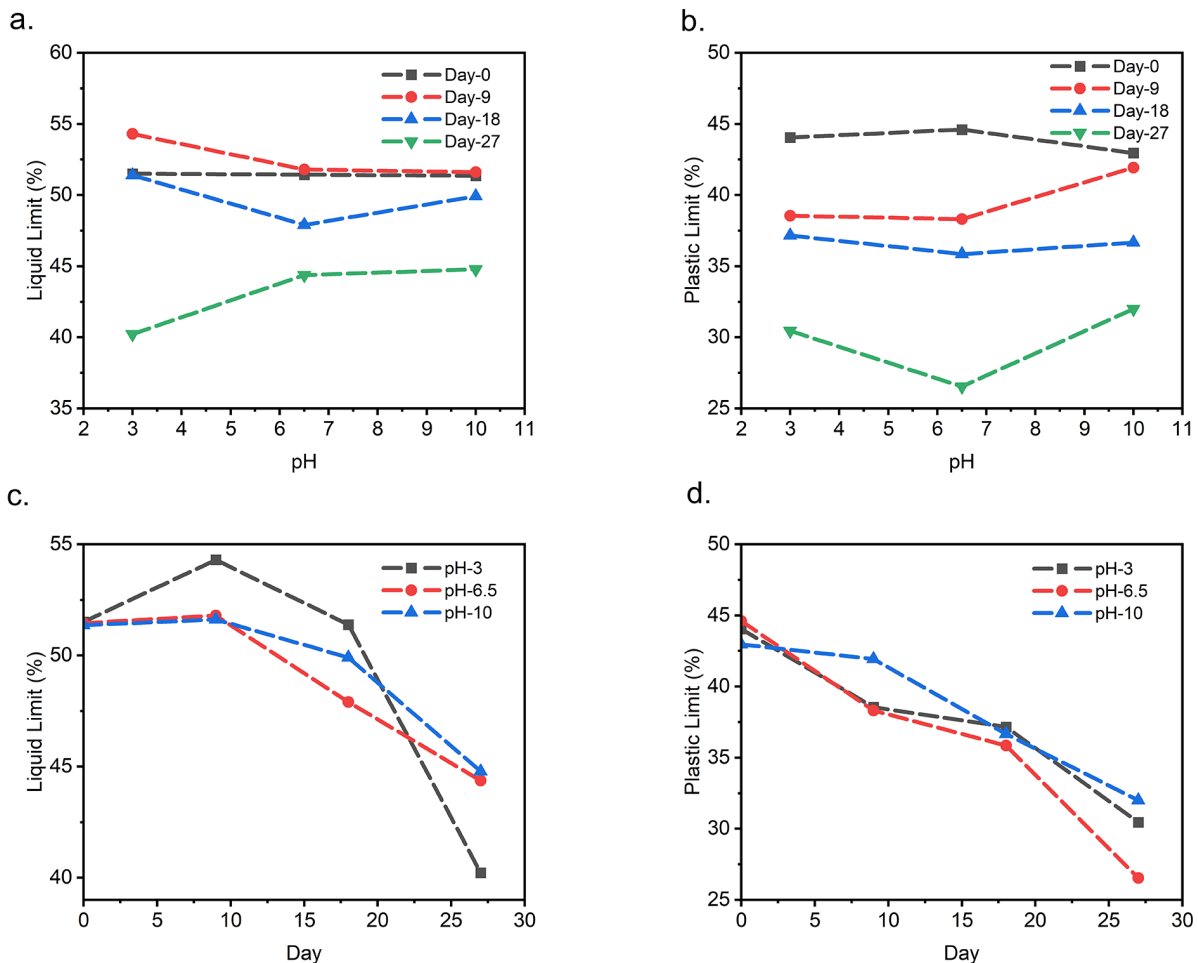


Figure 8. Variation of Atterberg limits (a) LL vs pH (b) PL vs pH (c) LL vs day (d) PL vs day

liquid limit and the plastic limit to decline. A similar reduction in Atterberg limits with the curing period was observed in some studies [Boardman et al., 2001; Nivedya, 2019; Rout & Singh, 2020]. Boardman et al. (2001) also found, when the curing time lengthens, English China clay’s liquid limit decreases. The dissolution of amorphous materials is associated with this declining tendency. Increasing the amount of amorphous materials will result in a soil system with high activity and low sensitivity [Yong et al., 1980]. The ability to store water increases with activity, hence the dissolution of amorphous materials decreased both the soil system’s capacity to hold water and its Atterberg limits.

Unconfined compressive strength tests

Figure 9 displays the strain vs. UCS for the sample’s 0, 9, 18, and 27 curing days, respectively. The brittle nature of the failure was obtained for all curing days when pore fluid is acidic and neutral, whereas, for alkaline pore fluid, ductile

nature was found to be developed after the ninth day of curing. Momeni et al. (2022) also found that when pH values were shifted to acidic and alkaline, the failure behaviour of the specimen was changed from brittle to ductile. In contrast to Momeni et al. (2022), the brittle failure of the specimen was obtained at acidic pore fluid in this study. The brittle failure thus obtained in acidic and neutral conditions must be due to the high presence of silica. According to Changizi & Haddad (2016), the extremely brittle behavior is exhibited by SiO_2 and the failure mechanism is initiated by the formation of tension cracks in cohesive soils. The adsorption of double layer water by nano- SiO_2 results in the formation of viscous gel when water is added to clay. The stronger bonding between clay particles can be expected due to viscous gel than absorbed water, which is also confirmed by peak strength results at neutral and acidic conditions obtained in this study. The dissolution of silica can occur at high pH ($pH > 8$) [Hoppe, 1986]. Al-Taie et al. (2018) have found a higher reduction in pH of lime treated basaltic

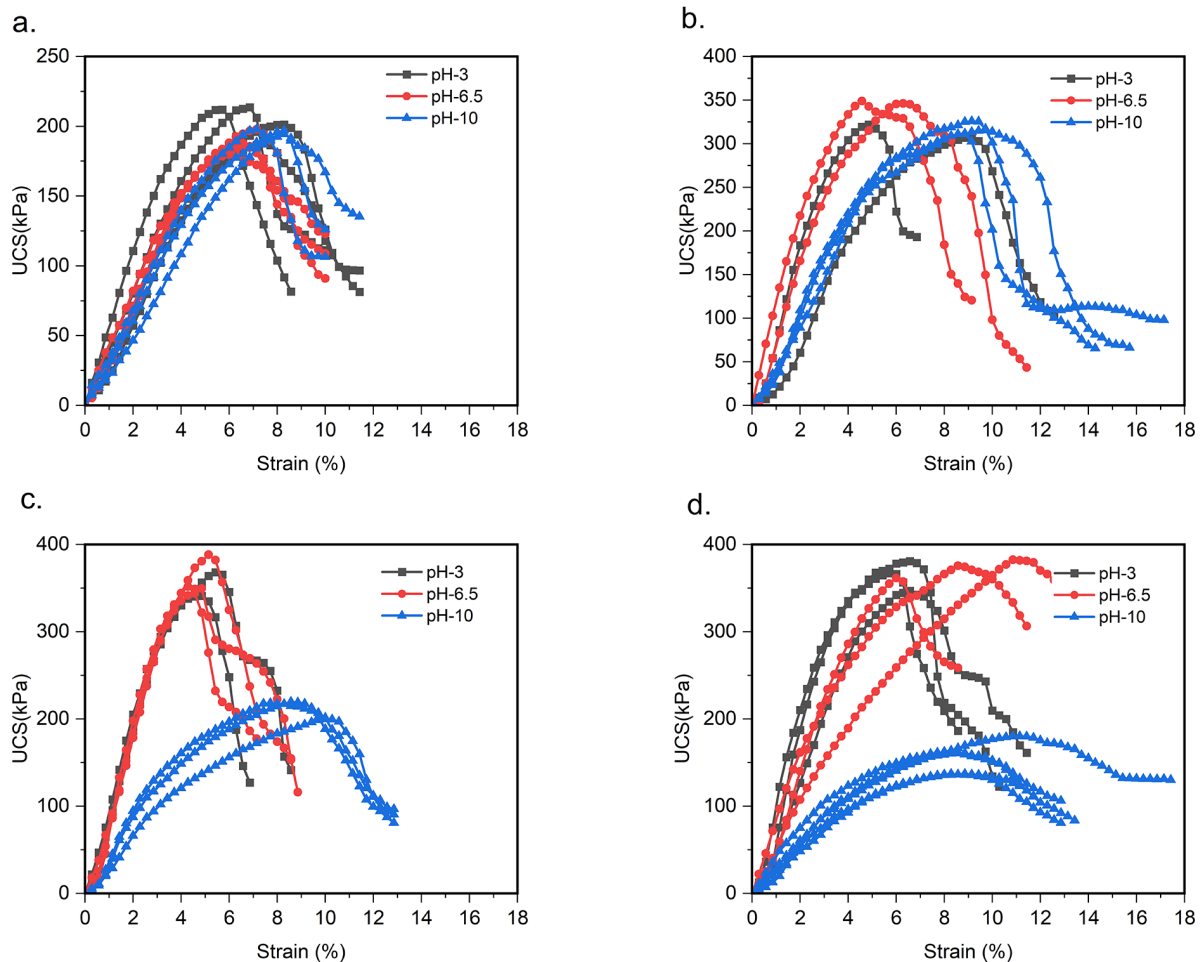


Figure 9 Stress-strain graph (a) 0 (b) 9 (c) 18 (d) 27 days

expansive clays in a curing period of 7 to 28 days, which was mainly due to consumption of OH⁻ for dissolution of silica. Based on the development of ductile nature of failure, reduction in peak strength in UCS test at alkaline conditions, and the results from aforementioned past studies, it can be stated that the dissolution of silica occurred at the later stage of curing in this study.

Unconfined compressive strength vs pH

The unconfined compressive strength varied with pH for different curing days which shown in Figure 10. The findings demonstrated that samples prepared with acidic and alkaline fluids had higher unconfined compressive strengths than samples produced with neutral fluids for samples that were tested instantly. Both acidic and alkaline conditions led to an increase in strength, but the acidic condition's increase was greater (8.5%) than the alkaline condition's (4.6%). This result is compatible with zeta potential results shown in Table 2. A high zeta potential suggests that the

double layer is more diffused [Aydin et al., 2004]. A high negative value of zeta potential for neutral conditions corresponds to lower strength than in acidic and alkaline conditions. Though zeta potential was measured after 27 days of curing, its good agreement with the UCS value of zero days showed that the changes in surface charge on clay particles and diffuse double layer thickness occurred initially. The diffuse double layer contracts as the cation concentration rises, increasing the inter-particle attraction that leads to the strength increase. The same trend of results was also obtained by some other researchers [Abedi Koupai et al., 2020; Ghobadi et al., 2014] on clay soil. Figure 11 shows the behaviour of soil in suspension in pore fluids of pH 3, 6.5, and 10 at 4 different elapsed times. There was a higher decrease in turbidity in acidic conditions than in neutral and alkaline conditions as the elapsed time increased. This showed the higher inter-particle attractive forces and particle aggregation in acidic conditions than in neutral and alkaline conditions, which corresponds to the higher instantaneous UCS at acidic conditions. On the 9th day of curing, the unconfined compressive strength decreased in both acidic and alkaline conditions in comparison to the neutral condition. The decrease in strength was more in acidic condition (11.9%) than in alkaline condition (8.6%). A similar trend was seen on the 18th and 27th days of curing with a greater decrease in strength in alkaline condition. The loss of cementing agents, such as iron or aluminium oxides & carbonates bonds, could be the cause of the strength decline during days 9, 18, and 27. For silty clay, Zanin et al. (2021) discovered a greater collapse index with acidic and alkaline fluids. While sodium-rich liquids tend to be dispersive to soils, breaking down the bonds between the particles and leading to higher deformation, acidic fluids may contribute to the

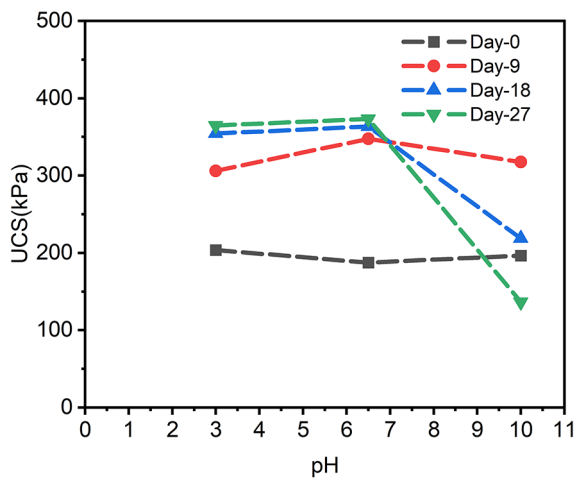


Figure 10. Unconfined compressive strength vs pH

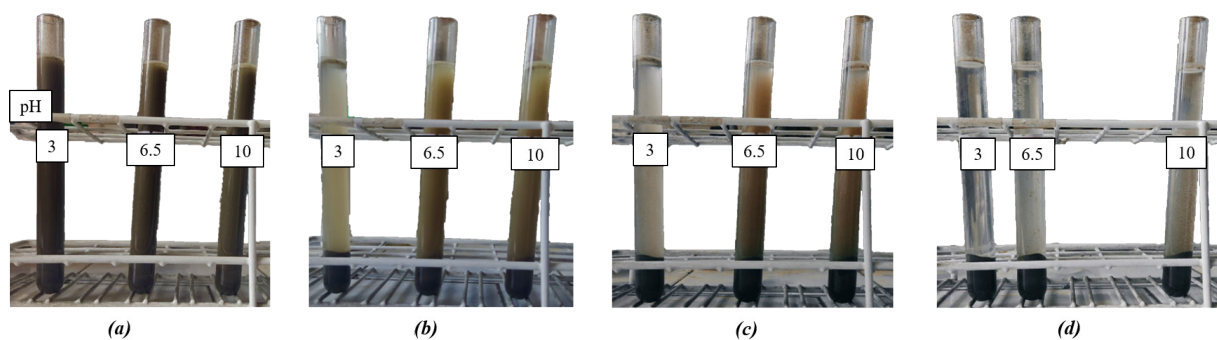


Figure 11. Soil solutions with acidic, neutral and alkaline pore fluid after (a) T=0 (b) T=30 min (c) 60 min (d) 24 hr

dissolution of carbonate, one of the substances responsible for maintaining the soil structure [Zanin et al., 2021]. Moreover, the cementing coating of silica and iron oxide is highly soluble in alkaline environments [Rao & Rao, 1994].

Unconfined compressive strength vs curing days

Figure 12 depicts the variations in the samples' unconfined compressive strength for various curing times and pH levels. For acidic and neutral conditions, the unconfined compressive strength increased with curing days. For alkaline conditions, there was an increase in strength up to 9th day and then a decrease in strength. The increase in strength for acidic and neutral followed the same trend i.e. rapid increase in strength up to 9th days and gradual increase in strength after that. For alkaline conditions, after the 9th day, strength decreased. The recovery of strength with curing days for acidic and neutral conditions is due to thixotropy. During remoulding, the initial structure is destroyed into a dispersed one, and the structure has a tendency to flocculate because the force field of interaction between attracting and repulsive forces in particles changes with time [Tang et al., 2021]. In soaking loess, silty soil in alkaline solutions, Xiu-juan et al. (2018) found a timely decrease in cohesion, whereas neutral and acidic solutions caused a timely increase in strength. Similar trend was obtained by Y. Li et al. (2021) on laterite when it is corroded by an alkaline solution. The results obtained in this study are in agreement with previous studies. An alkaline solution dispersed the soil because of the sodium concentration and high pH [Fan & Kong, 2013].

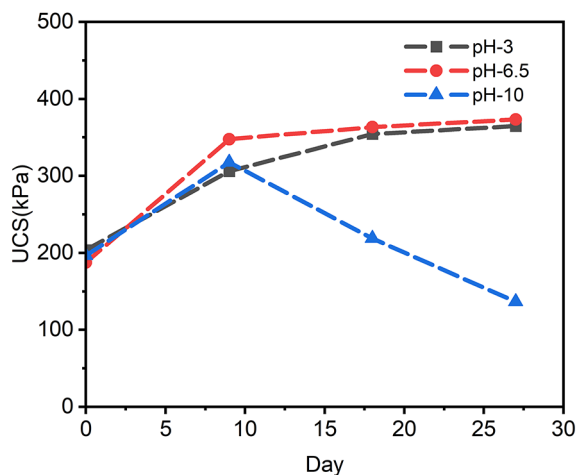


Figure 12. UCS vs curing days

CONCLUSIONS

On different curing days, the impact of pore fluid pH was examined on the soil's particle size distribution, Atterberg limits, and unconfined compressive strength. After 27 days of curing, zeta potential was also assessed. On the basis of the outcomes, the following conclusions can be drawn:

1. The particle size distribution of the soil was affected differentially by the various pH values. Lower silt fractions in alkaline conditions and lower clay fractions in acidic conditions were obtained. These alterations are related to variations in DDL thickness and alumina's chemical dissolution under various pH settings.
2. Atterberg limits were found to be significantly affected by pH and curing days. These decreased with curing days. A higher liquid limit was obtained at low or high pH for curing days 9 and 18. The opposite trend was obtained for 27 curing days. A high plastic limit was obtained at low or high pH for all curing days. Increase in manipulation, dissolution of cementitious materials from soil structure, and shrinkage of the diffuse double layer are some phenomena that are attributed to these changes.
3. Unconfined compressive strength was also found to be affected by pH and curing days. An instant increase in strength was seen with acidic or alkaline pore fluid but the long-term strength decreased due to the dissolution of cementitious materials, the reduction being higher in alkaline conditions. This reduction is attributed to the dissolution of amorphous material at higher pH. Soil, being a complex system, exhibits different phenomena responsible for changes in its properties due to pH variation of pore fluid, necessitating more detailed study.

Acknowledgements

The Department of Civil Engineering at the Pulchowk Campus is to be thanked for supporting our effort and supplying the essential materials. The authors are exceedingly appreciative to Er. Ujjwal Niraula's dynamic recommendations as well as Dr. Tista Prasai's and Ms. Naina Byanjankar's help in measuring Zeta Potential.

REFERENCES

1. Abdullah W.S., Alshibli K.A., Al-Zou'bi M.S. 1999. Influence of pore water chemistry on the swelling behavior of compacted clays. *Applied Clay Science*, 15(5), 447–462. [https://doi.org/10.1016/S0169-1317\(99\)00034-4](https://doi.org/10.1016/S0169-1317(99)00034-4)
2. Abedi Koupai J., Fatahizadeh M., Mosaddeghi M.R. 2020. Effect of pore water pH on mechanical properties of clay soil. *Bull Eng Geol Environ*, 79(3), 1461–1469. <https://doi.org/10.1007/s10064-019-01611-1>
3. Al-Omari R.R., Mohammed W.K., Nashaat I.H., Kaseer O.M. 2007. Effect of sulphuric and phosphoric acids on the behaviour of a limestone foundation. *Indian Geotechnical Journal*, 37(4), 263–282.
4. Al-Taie A., Disfani M., Evans R., Arulrajah A., Horpibulsuk S. 2018. Impact of curing on behaviour of basaltic expansive clay. *Road Materials and Pavement Design*, 19(3), 624–645. <https://doi.org/10.1080/14680629.2016.1267660>
5. Ashfaq M., Heeralal M., Hari Prasad Reddy P. 2019. A study on strength behavior of alkali-contaminated soils treated with fly ash. *Lecture Notes in Civil Engineering*, 32, 137–143. Springer. https://doi.org/10.1007/978-981-13-7017-5_16
6. Assa'ad A. 1998. Differential upheaval of phosphoric acid storage tanks in Aqaba, Jordan. *Journal of Performance of Constructed Facilities*, 12(2), 71–76.
7. Aydin M., Yano T., Kilic S. 2004. Dependence of zeta potential and soil hydraulic conductivity on adsorbed cation and aqueous phase properties. *Soil Science Society of America Journal*, 68(2), 450–459. <https://doi.org/10.2136/sssaj2004.4500>
8. Bakhshipour Z., Asadi A., Huat B.B.K., Sridharan A., Kawasaki S. 2016. Effect of acid rain on geotechnical properties of residual soils. *Soils and Foundations*, 56(6), 1008–1020. <https://doi.org/10.1016/j.sandf.2016.11.006>
9. Boardman D.I., Glendinning S., Rogers C.D.F. 2001. Development of stabilisation and solidification in lime-clay mixes. *Geotechnique*, 51(6), 533–543. <https://doi.org/10.1680/geot.2001.51.6.533>
10. Changizi F., Haddad A. 2016. Effect of nano-SiO₂ on the geotechnical properties of cohesive soil. *Geotech Geol Eng*, 34(2), 725–733. <https://doi.org/10.1007/s10706-015-9962-9>
11. Chorom M., Rengasamy P. 1995. Dispersion and zeta potential of pure clays as related to net particle charge under varying pH, electrolyte concentration and cation type. *European Journal of Soil Science*, 46(4), 657–665.
12. Das. 2010. *Principles of Geotechnical Engineering*. Cengage Learning India Private Limited.
13. Fan H., Kong L. 2013. Empirical equation for evaluating the dispersivity of cohesive soil. *Canadian Geotechnical Journal*, 50(9), 989–994. <https://doi.org/10.1139/cgj-2012-0332>
14. Ghobadi M.H., Abdilor Y., Babazadeh R. 2014. Stabilization of clay soils using lime and effect of pH variations on shear strength parameters. *Bulletin of Engineering Geology and the Environment*, 73(2), 611–619. <https://doi.org/10.1007/s10064-013-0563-7>
15. Gratchev I., Towhata I. 2013. Stress–strain characteristics of two natural soils subjected to long-term acidic contamination. *Soils and Foundations*, 53(3), 469–476. <https://doi.org/10.1016/j.sandf.2013.04.008>
16. Hoppe E. 1986. *The Influence of Acid Rain on the Engineering Properties of a Sensitive Clay*. McGill University (Canada).
17. IS:2720–10. 1973. *Methods of test for soil part 10: Determination of unconfined compressive strength (first revision)*. Bureau of Indian Standards.
18. IS:2720–26. 1987. *Methods of test for soils part 26: Determination of pH value*. Bureau of Indian Standards.
19. IS:2720–3/1. 1980. *Methods of test for soils, Part 3/ Section 1: Determination of specific gravity of fined grained soils*. Bureau of Indian Standards.
20. IS:2720–4. 1985. *Methods of test for soils part 4: grain size analysis*. Bureau of Indian Standards.
21. IS:2720–5. 1985. *Methods of test for soils part 5: Determination of liquid and plastic limit*. Bureau of Indian Standards.
22. IS 1498. 1970. *Indian Standard Code of Practice for Soil Classification*. 3rd Edition, Bureau of Indian Standards, New Delhi. – References – Scientific Research Publishing. [https://www.scirp.org/\(S\(i43dyn45teexjx455qlt3d2q\)\)/reference/ReferencesPapers.aspx?ReferenceID=2123098](https://www.scirp.org/(S(i43dyn45teexjx455qlt3d2q))/reference/ReferencesPapers.aspx?ReferenceID=2123098)
23. Ismail A.F., Khulbe K.C., Matsuura T. 2019. Chapter 3 – RO Membrane Characterization. In A. F. Ismail, K.C. Khulbe, & T. Matsuura (Eds.), *Reverse Osmosis* (pp. 57–90). Elsevier. <https://doi.org/10.1016/B978-0-12-811468-1.00003-7>
24. Kamon M., Ying C., Katsumi T. 1997. Effect of acid rain on physico-chemical and engineering properties of soils. *Soils and Foundations*, 37(4), 23–32.
25. Khodabandeh M.A., Nokande S., Besharatinezhad A., Sadeghi B., Hosseini S.M. 2020. The effect of acidic and alkaline chemical solutions on the behavior of collapsible soils. *Periodica Polytechnica Civil Engineering*, 64(3), 939–950. <https://doi.org/10.3311/PPci.15643>
26. Kiros F., Shakya K.M., Rupakheti M., Regmi R.P., Maharjan R., Byanju R.M., Naja M., Mahata K., Kathayat B., Peltier R.E. 2016. Variability of

- anthropogenic gases: nitrogen oxides, sulfur dioxide, ozone and ammonia in Kathmandu Valley, Nepal. *Aerosol Air Qual. Res.*, 16(12), 3088–3101. <https://doi.org/10.4209/aaqr.2015.07.0445>
27. Lessard G., Mitchell J.K. 1985. The causes and effects of aging in quick clays. *Can. Geotech. J.*, 22(3), 335–346. <https://doi.org/10.1139/t85-046>
 28. Li Y., Luo Y., Hu S., Gao J., Wang C. 2021. Effect of alkali seepage erosion on physical and mechanical properties of laterite. *Advances in Materials Science and Engineering*, 2021. <https://doi.org/10.1155/2021/8002984>
 29. Liu H., He J., Zhao Q., Wang T. 2021. An experimental investigation on engineering properties of undisturbed loess under acid contamination. *Environmental Science and Pollution Research*, 28(23), 29845–29858.
 30. Lowry G.V, Hill R.J., Harper S., Rawle A.F., Hendren C.O., Klaessig F., Nobbmann U., Sayre P., Rumble J. 2016. Guidance to improve the scientific value of zeta-potential measurements in nanoEHS. *Environmental Science: Nano*, 3(5), 953–965.
 31. Mahapatra P.S., Puppala S.P., Adhikary B., Shrestha K.L., Dawadi D.P., Paudel S.P., Panday A.K. 2019. Air quality trends of the Kathmandu Valley: A satellite, observation and modeling perspective. *Atmospheric Environment*, 201, 334–347.
 32. Matsumoto S., Ogata S., Shimada H., Sasaoka T., Hamanaka A., Kusuma G.J. 2018. Effects of pH-induced changes in soil physical characteristics on the development of soil water erosion. *Geosciences*, 8(4), 134. <https://doi.org/10.3390/geosciences8040134>
 33. Mitchell J.K., Soga K. 2005. *Fundamentals of soil behavior* (Vol. 3). John Wiley & Sons New York.
 34. Momeni M., Bayat M., Ajalloeian R. 2022. Laboratory investigation on the effects of pH-induced changes on geotechnical characteristics of clay soil. *Geomechanics and Geoen지니어ing*, 17(1), 188–196.
 35. Nikhil John K., Arnepalli D.N. 2019. Factors influencing zeta potential of clayey soils. In: V.K. Stalin & M. Muttharam (Eds.), *Geotechnical Characterisation and Geoenvironmental Engineering*, pp. 171–178. Springer. https://doi.org/10.1007/978-981-13-0899-4_21
 36. Nivedya K. 2019. study on the effect of pH on the atterberg limits of kaolinitic and montmorillonitic clay. In *Lecture Notes in Civil Engineering* (Vol. 16, pp. 251–256). Springer. https://doi.org/10.1007/978-981-13-0899-4_31
 37. Ogner G., Randem G., Remedios G., Wickstrøm T. 2001. Increase of soil acidity and concentrations of extractable elements by 1 m ammonium nitrate after storage of dry soil for up to 5 years at 22°C. *Communications in Soil Science and Plant Analysis*, 32(5–6), 675–684. <https://doi.org/10.1081/CSS-100103900>
 38. Ola S.A. 1980. Mineralogical properties of some nigerian residual soils in relation with building problems. *Engineering Geology*, 15(1–2), 1–13. [https://doi.org/10.1016/0013-7952\(80\)90027-7](https://doi.org/10.1016/0013-7952(80)90027-7)
 39. Osuolale O.M., Falola O.D., Ayoola M.A. 2012. Effect of pH on geotechnical properties of laterite soil used in highway pavement construction. *Civil and Environmental Research*, 2(10), 23–28.
 40. Prodromou K.P., Pavlatou-Ve A.S. 1998. Changes in soil pH due to the storage of soils. *Soil Use and Management*, 14(3), 182–183. <https://doi.org/10.1111/j.1475-2743.1998.tb00146.x>
 41. Rao S.M., Rao K.S.S. 1994. Ground heave from caustic soda solution spillage – a case study. *Soils and Foundations*, 34(2), 13–18. https://doi.org/10.3208/sandf1972.34.2_13
 42. Ratnaweera P., Meegoda J. 2006. Shear strength and stress-strain behavior of contaminated soils. *Geotechnical Testing Journal*, 29. <https://doi.org/10.1520/GTJ12686>
 43. Rodríguez-Eugenio N., McLaughlin M., Pennock D. 2018. Soil pollution: a hidden reality. <http://www.fao.org/3/i9183en/I9183EN.pdf>
 44. Rout S., Singh S.P. 2020. Effect of inorganic salt solutions on physical and mechanical properties of bentonite based liner. *Journal of Hazardous, Toxic, and Radioactive Waste*, 24(4). [https://doi.org/10.1061/\(asce\)hz.2153-5515.0000553](https://doi.org/10.1061/(asce)hz.2153-5515.0000553)
 45. Salopek B., Krasic D., Filipovic S. 1992. Measurement and application of zeta-potential. *Rudarsko-Geolosko-Naftni Zbornik*, 4(1), 147.
 46. Santamarina J.C., Klein K.A., Palomino A., Guimaraes M.S. 2001. Micro-scale aspects of chemical-mechanical coupling–interparticle forces and fabric. *Chemo-Mechanical Coupling in Clays: From Nano-Scale to Engineering Applications*, 47–64. <https://www.taylorfrancis.com/chapters/edit/10.1201/9781315139289-3/micro-scale-aspects-chemical-mechanical-coupling-interparticle-forces-fabric-santamarina-klein-palomino-guimaraes>
 47. Schwarzenbach R.P., Egli T., Hofstetter T.B., Von Gunten U., Wehrli B. 2010. Global water pollution and human health. *Annual Review of Environment and Resources*, 35, 109–136. <https://doi.org/10.1146/annurev-environ-100809-125342>
 48. Shang J.Q. 1997. Zeta potential and electroosmotic permeability of clay soils. *Can. Geotech. J.*, 34(4), 627–631. <https://doi.org/10.1139/t97-28>
 49. Shrestha S., Prasad Pandey V., Yoneyama Y., Shrestha S., Kazama F. 2013. An evaluation of rainwater quality in Kathmandu Valley, Nepal. *Sustainable Environment Research*, 23(5).
 50. Sivapullaiah P.V. 2015. Surprising soil behaviour: Is it really! *Indian Geotech J*, 45(1), 1–24.

- <https://doi.org/10.1007/s40098-014-0141-3>
51. Spagnoli G., Rubinos D., Stanjek H., Fernández-Steegeer T., Feinendegen M., Azzam R. 2012. Undrained shear strength of clays as modified by pH variations. *Bull Eng Geol Environ*, 71(1), 135–148. <https://doi.org/10.1007/s10064-011-0372-9>
 52. Sunil B.M., Nayak S., Shrihari S. 2006. Effect of pH on the geotechnical properties of laterite. *Engineering Geology*, 85(1), 197–203. <https://doi.org/10.1016/j.enggeo.2005.09.039>
 53. Tang B., Zhou B., Xie L., Yin J. 2021. Evaluation method for thixotropy of clay subjected to unconfined compressive test. *Frontiers in Earth Science*, 9. <https://www.frontiersin.org/articles/10.3389/feart.2021.683454>
 54. Umesha T.S., Dinesh S.V., Sivapullaiah P.V. 2012. Effects of acids on geotechnical properties of black cotton soil. *International Journal of Geology*, 6(3), 69–76.
 55. Xiu-juan Y., Heng-hui F. A.N., Cheng C., Ying-jia Y.A.N., Re-mei L.I.U. 2018. Effects of the pore water's pH value on the shear strength of the Loess.
 56. Xu P., Zhang Q., Qian H., Yang F., Zheng L. 2021. Investigating the mechanism of pH effect on saturated permeability of remolded loess. *Engineering Geology*, 284, 105978. <https://doi.org/10.1016/j.enggeo.2020.105978>
 57. Yang F., Tan J., Shi Z. B., Cai Y., He K., Ma Y., Duan F., Okuda T., Tanaka S., Chen G. 2012. Five-year record of atmospheric precipitation chemistry in urban Beijing, China. *Atmospheric Chemistry and Physics*, 12(4), 2025–2035. <https://doi.org/10.5194/acp-12-2025-2012>
 58. Yong R.N., Sethi A.J., Suzuki A. 1980. Contribution of amorphous material to properties of a laboratory-prepared soil. *Can. Geotech. J.*, 17(3), 440–446. <https://doi.org/10.1139/t80-050>
 59. Yue J., Chen Y., Luo Z., Wang S., Su H., Gao H., Li Y., Li P., Ma C. 2022. Experimental study on effects of aging time on dry shrinkage cracking of lime soils. *Materials*, 15(16). <https://doi.org/10.3390/ma15165785>
 60. Yukselen Y., Kaya A. 2003. Zeta potential of kaolinite in the presence of alkali, alkaline earth and hydrolyzable metal ions. *Water, Air, & Soil Pollution*, 145(1), 155–168. <https://doi.org/10.1023/A:1023684213383>
 61. Zanin R.F.B., Padilha A.C.C., Pelaquim F.G.P., Gutierrez N.H.M., Teixeira R.S. 2021. The effect of pH and electrical conductivity of the soaking fluid on the collapse of a silty clay. *Soil. Rocks*, 44. <https://doi.org/10.28927/SR.2021.061620>
 62. Zeng J., Yue F.J., Li S.L., Wang Z.J., Wu Q., Qin C.Q., Yan Z.L. 2020. Determining rainwater chemistry to reveal alkaline rain trend in Southwest China: Evidence from a frequent-rainy karst area with extensive agricultural production. *Environmental Pollution*, 266, 115166. <https://doi.org/10.1016/J.ENVPOL.2020.115166>